Biophysical Chemistry 145 (2009) 72–78

Contents lists available at ScienceDirect

Biophysical Chemistry

journal homepage: http://www.elsevier.com/locate/biophyschem

Membrane-induced peptide structural changes monitored by infrared and circular dichroism spectroscopy

Daniel J. Laird, Melinda M. Mulvihill, Jennifer A. Whiles Lillig *

Department of Chemistry, Sonoma State University, 1801 East Cotati Avenue, Rohnert Park, CA 94928, United States

ARTICLE INFO

Article history:
Received 20 July 2009
Received in revised form 3 September 2009
Accepted 4 September 2009
Available online 12 September 2009

Keywords:
Infrared spectroscopy
Circular dichroism
Membrane peptide structure
Mastoparan X
Gramicidin
Leucine enkephalin

ABSTRACT

As more peptide secondary structures deduced by infrared spectroscopy (IR) have been reported in the literature, there have been overlaps in assignments of elements of secondary structure to carbonyl vibrational frequencies. We have investigated this phenomenon with regards to the use of IR for monitoring membrane-induced structural changes using conformationally diverse peptides. These IR studies, complemented by circular dichroism (CD) experiments, revealed that peptide–solvent interactions can mask membrane-induced conformational changes monitored by IR. A structural transition from random coil to α-helix upon the binding of mastoparan X to a membrane was clearly observed by CD but obscured in the amide I region of the IR spectrum. In addition, unlike the buried helical peptides gramicidin D and P16 in micelles, the amide II peak for mastoparan X was absent, likely due to H–D exchange. This suggests information on the peptide's membrane-bound solvent accessibility could be obtained from this region of the spectrum.

1. Introduction

Infrared spectroscopy (IR) provides an opportunity to quickly obtain structural information on peptides and proteins in a variety of different chemical environments. This is potentially useful for examining the partitioning features of membrane active peptides. Since the biological activity of these peptides can depend directly on the lipid composition of the membrane bilayer, IR can provide an easily accessible and simple method for monitoring the effects of lipid composition on protein conformation. IR for structural analysis of small peptides is particularly advantageous since there is likely only a minimal amount of secondary structure within the molecule, resulting in simpler spectra that should not require high degrees of spectral deconvolution for interpretation. However, previous studies have shown that the analysis of protein IR spectra to deduce contributions from different forms of secondary structure must be approached with caution [1,2]. 2D IR spectroscopy is also being introduced as a new method to circumvent some of the inherent ambiguities in 1D spectra [3,4].

In IR, the amide I band (approximately 1600–1700 cm^{-1}) resulting from the CO stretching vibration has been shown to be the most sensitive to backbone conformation and the amide II band (approximately 1510–1580 cm^{-1}) resulting from the N–H bending vibration coupled to the C–N stretching vibration has also been suggested to be somewhat sensitive to protein secondary structure [5–12]. This latter band is suggested to be even more sensitive to the protonation state of the amide nitrogen [13]. Although specific amide I, and sometimes amide II, bands have been assigned to distinctive types of secondary structure, these characteristic frequencies sometimes overlap which could result in mis-assignment of the band. In order to provide further insight into the interpretation of IR data for small peptides, we have methodically used IR and circular dichroism (CD) spectroscopy to compare the structures of four structurally diverse membrane-associating peptides in different chemical environments. All peptides in this work have been previously studied in different solvents by various spectroscopic methods including CD, NMR, X-ray crystallography, and to some extent, IR. Of the peptides in this study, leucine enkephalin (Leu-Enk), gramicidin (Gram), and to a lesser extent mastoparan X (MPX) have been characterized by IR in some solvents, while P16 has not.

Leu-Enk (Tyr-Gly-Gly-Phe-Leu), a small peptide hormone with morphine-like activity, has been shown to form β-type structures in a variety of different solvents. However, the precise nature of these structures (β-sheet, β-turn, β-bend) has been controversial over the years and has been suggested to be dependent upon environmental factors such as overall peptide charge and nature of the solvent system [14–18]. GramD (L-Val-Gly-L-Ala-D-Leu-L-Ala-D-Val-L-Val-D-Val-L-Trp-D-Leu-L-Trp-D-Leu-L-Trp-D-Leu-L-Trp), an antimicrobial peptide from *Bacillus brevis*, is a heterogeneous mixture of pentadecapeptides with conservative variations in the hydrophobic amino acids at positions 1

Abbreviations: CD, circular dichroism spectroscopy; DCPC, dicaproylphosphatidylcholine; DMPC, dimyristoylphosphatidylcholine; DTPC, ditetradecylphosphatidylcholine; Gram, gramicidin; GramA, gramicidin A; GramD, gramicidin D; IR, infrared spectroscopy; Leu-Enk, leucine enkephalin; MPX, mastoparan X; MeOH, methanol; MLV, multilamellar vesicle; TFA, trifluoroacetic acid; TFE, trifluoroethanol.

* Corresponding author. Tel.: +1 707 664 2331; fax: +1 707 664 3378.
E-mail address: Jennifer.Whiles@sonoma.edu (J.A. Whiles Lillig).

0301-4622/$ – see front matter © 2009 Elsevier B.V. All rights reserved.
doi:10.1016/j.bpc.2009.09.002

and 11. Structural studies on GramA, a component of GramD, have suggested that the molecule is dimeric with several different oligomerized hydrogen-bonded forms. These differences in oligomerization are thought to be a function of environment as well as a reflection of different functional states of the peptide [19].

P16 (Ac-Lys-Lys-Gly-$(Leu)_7$-Ala-$(Leu)_7$-Lys-Lys-Ala-NH_2) is an engineered lysine-flanked polyleucine peptide that has been shown to form a stable, hydrophobic transmembrane α-helix in a model membrane environment [20]. P16, like GramD, is not soluble in aqueous solution. MPX (Ile-Asn-Trp-Lys-Gly-Ile-Ala-Ala-Met-Ala-Lys-Lys-Leu-Leu-NH_2), a channel-forming peptide from wasp venom, has been shown to be random coil in aqueous solution and to assume an amphipathic α-helical conformation (from residues 3–14) in the presence of micelles, bicelles, or other membrane-mimetic solvents like trifluoroethanol (TFE) [21–24]. Although they have the same secondary conformation, unlike P16, MPX has been shown to associate at the membrane interface of zwitterionic bilayers [23]. These two latter peptides will therefore allow for direct comparison of effects of solvent and mechanism of membrane-association on the IR spectrum.

In this work, the secondary structure of these four membrane-binding peptides was studied by IR and CD in the presence and absence of different membrane-mimetics. Solvents examined for each peptide were chosen based on peptide solubility, for comparison to previous work, and to allow for comparison of the effect of aqueous vs membrane-like systems on peptide conformation. The membrane-mimetic solvents (alcohols, micelles, bilayers) have been shown to induce structure in these peptides and can therefore be used to examine solvent effects on the IR spectrum when the same secondary structure is present; this was particularly important in the examination of MPX. Results are compared to previous structural analyses by IR and additional spectroscopic methods. Consequences for the use of IR spectroscopy in adequately probing membrane-induced structural changes will be discussed.

2. Experimental

2.1. Materials

Leu-Enk, GramD, and spectroscopy solvents were purchased from Sigma-Aldrich (St. Louis, MO) and MPX was obtained from Bachem (King of Prussia, PA). P16 was synthesized using standard FMOC chemistry on a MilliGen 9050 solid-state peptide synthesizer and purified by high performance liquid chromatography following previously described procedures [20]. Dicaproylphosphatidylcholine (DCPC) and dimyristoylphosphatidylcholine (DMPC) were obtained from Avanti Polar Lipids (Alabaster, AL). All purchased chemicals and solvents were used without further purification.

2.2. IR

All samples for infrared spectroscopy were prepared by dissolving the peptides in the appropriate solvent (D_2O, alcohol, 5 mM DCPC monomers, 20 mM and greater concentration DCPC micelles [25] prepared in D_2O (pH 7.1)). Concentrations were chosen based on instrument sensitivity and a final concentration of 1.5 mg peptide/mL yielded suitable signal/noise ratios for all peptides. This corresponded to: 1 mM MPX, 0.6 mM P16, 2.7 mM Leu-Enk, and 0.8 mM GramD. Additional samples with 15 mg/mL (27 mM) Leu-Enk were also examined. The pH of the peripheral membrane peptides ranged from 4.7 to 4.9 for aqueous Leu-Enk samples and 4.4 to 6.0 for aqueous MPX samples. Additional samples of Leu-Enk in DMPC multilamellar vesicles (MLVs) were prepared using a 15:1 lipid:peptide weight ratio as described previously [15]. Background subtracted spectra were obtained on a Perkin-Elmer Spectrum 1000 FT-IR spectrometer using CaF_2 windows. Each spectrum was acquired at room temperature with 300 scans at a resolution of 2 cm^{-1}. Absorbance numbers were converted to molar absorptivity for each spectrum and plotted using Igor Pro 5.04B. Spectra were smoothed using a 2nd order 13-point Savitsky–Golay function.

2.3. CD

Samples for CD spectroscopy were prepared by dissolving the peptide in each solvent system at concentrations based on instrument sensitivity. Resulting concentrations were: 1 mM MPX in H_2O and 0.4 mM MPX in all other solvents, 0.4 mM P16 in all solvent systems, 1 mM Leu-Enk in H_2O and 484 mM DCPC micelles and 0.07 mM Leu-Enk in 20 mM DCPC micelles, and 84 μM GramD in all solvent systems. The pH of DCPC micelles was 5.2 and the final pH values of the peripheral membrane peptides ranged from 4.4 to 4.9 for aqueous Leu-Enk samples and 6.2 to 6.7 for aqueous MPX samples. Spectra were obtained on an Aviv Model 215 circular dichroism spectrometer equipped with a Peltier-type thermoelectric cell holder using a 1 mm path quartz cuvette. Spectra were acquired in 1.0 nm intervals. Background was subtracted prior to conversion to molar ellipticity.

3. Results

3.1. IR assignments

Table 1 shows some characteristic frequencies in the amide I and amide II regions of the IR spectrum that have commonly been used as reference points for structural assignments. However, these frequency ranges are sometimes close together or overlap significantly. For example, as shown in Table 1, a band at 1640–1645 cm^{-1} has been assigned to both antiparallel β-sheet and random coil conformation in aqueous solution. It is also not uncommon for a given secondary structure to result in a frequency outside of these ranges. Shifts in characteristic amide I frequencies have been observed due to solvent interaction or membrane-association even though the peptides maintained the same secondary structure under different conditions. For example, studies in Table 1 have shown that a peak at 1650 cm^{-1} is characteristic of a buried α-helix in proteins whereas this peak is shifted to around 1632 cm^{-1} for solvated α-helices. These differences are thought to arise from changes in hydrogen bonding patterns

Table 1
Previously determined characteristic IR frequencies as a function of secondary structure.

Frequency (cm^{-1})	Secondary structure	Source
Amide I		
1620–1640	β-sheet(parallel, antiparallel)	[5,31]
1675 ± 4	β-sheet(antiparallel)	[5,31]
1615–1637, 1696	β-sheet	[42]
1640	β-sheet(antiparallel)	[42]
1630(strong) + 1680(weak)	β-sheet(antiparallel)	[10]
1645 ± 4	Random coil	[5,31,43]
1650	α-helix	[9]
1652	α-helix	[44]
1655 ± 4	α-helix	[5]
1650–1658	α-helix	[13,45]
1660–1670, 1680–1696	β-turn	[5,31]
1680	β-turn	[13]
Amide II		
1547	β-sheet	[14]
1548	α-helix	[44]
1550(strong) + 1530(weak)	β-turn	[37]
Membrane-associated Amide I		
1610–1628	β-sheet	[1]
1640–1645	Random coil	[1]
1650–1655	Buried α-helix	[1]
1632	Solvated α-helix	[46–48]
1656–1670	3^{10} helix	[1]
1670–1680	β-turn	[49]

between the peptide and surrounding solvent [26–28] and this phenomenon has been used to probe the interaction of membrane-associating peptides with bilayers [29]. However, the 1632 cm^{-1} assignment for solvated α-helices overlaps with the range reported for amide I stretches of aqueous β-sheets so it may become difficult to separate spectral features arising from peptide conformation vs. membrane-association.

3.2. Leu-Enk

As shown in Fig. 1A, CD spectra of Leu-Enk in water and 20 mM DCPC micelles were the same shape with maxima near 200 nm and 220 nm. These spectra were similar in shape to previous CD spectra of glycosylated enkephalins in water [30]. The band at 220 nm is suggestive of random coil conformation while the band at 200 nm could be due to either beta-type structure or alpha helical structure; the former contribution is more likely based on previous work [14–18]. Increasing the concentration of DCPC to 484 mM (Fig. 1B) resulted in a distinctive spectral change with a decrease in molar ellipticity near 200 nm and a more negative molar ellipticity near 220 nm. The contribution of multiple secondary conformations makes it difficult to deconvolute these spectra to obtain more detailed structural information but the spectral difference between Leu-Enk in water and 484 mM DCPC micelles suggests a change in the distribution of structures sampled by Leu-Enk upon membrane-association.

For comparison to current IR data, Table 2 shows previous IR studies of Leu-Enk in various solvents. IR studies of 27 mM Leu-Enk in buffer and MLVs composed of ditetradecylphosphatidylcholine (DTPC), an ether linked phospholipid, demonstrated a shift in maximum intensity suggestive of a conformational change upon binding of the peptide to the membrane surface [15]. In these studies, the appearance of a 1664 cm^{-1} peak coincided with the disappearance of a peak at 1643 cm^{-1}, suggesting that the lipid-induced turn structure was achieved for peptides that were previously in a random coil conformation. The complete absence of the 1643 cm^{-1} peak in the original 1985 study [14] was attributed by the 1988 authors [15] to the fact that the original study was an ATR–FT-IR analysis and that the observed IR signal was due primarily to peptide absorbed on the plate in a distinct conformation rather than from a distribution of peptide in the water. However, it should also be noted that the orientation of the incident laser with respect to the axis of the secondary structure in IR-ATR studies plays an important factor in the observed spectra and may be responsible for the absence of the 1643 cm^{-1} peak. Furthermore, although the IR spectra in the 1985 and 1988 studies both had peaks at 1658 cm^{-1} and 1652 cm^{-1}, respectively, an assignment of this peak to α-helical structure was not supported by other spectroscopic studies. "Phantom peaks" such as this have been seen in other studies as well [31,32].

Table 2
Previously determined characteristic IR peaks for leucine enkephalin and gramicidin A.

Peptide	Frequency (cm^{-1})	Assignment	Solvent	Source
Leu-Enk	Amide I		H_2O	[14]
	1632	β-sheet		
	1675(sh)	β-sheet		
	1663	β-turn (Type II)		
	1658(sh)	Undetermined		
	Amide II			
	1547	β-sheet		
	Amide I		MES pH 6, D_2O	[15]
	1626	β-strand		
	1643	Solvated backbone; random coil		
	1652	Atypical, nonperiodic structure		
	1680	β-turn		
	Amide I		DTPC MLV	[15]
	1624	β-strand		
	1653	Atypical, nonperiodic structure		
	1664	β-turn		
	1680	β-turn		
GramA	Amide I		$CHCl_3$	[37]
	1633	β-sheet		
	1650(sh)	Unassigned		
	1680	β-type H-bonds		
	Amide II			
	1545	Unassigned		
	Amide I		Lysolecithin bilayer	[38]
	1633	Single stranded β-helix		

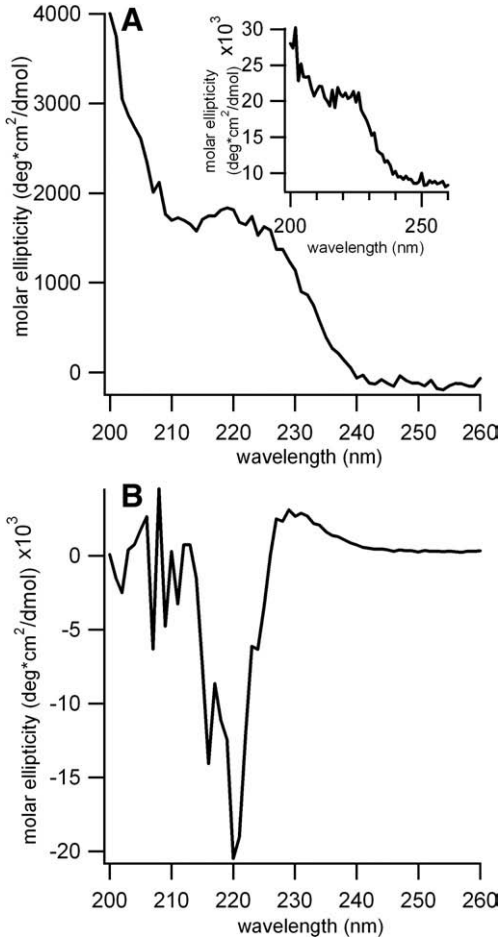

Fig. 1. CD spectra of A) 1 mM Leu-Enk in water and 0.07 mM Leu-Enk in 20 mM DCPC micelles (inset) and B) 1 mM Leu-Enk in 484 mM DCPC micelles.

Our IR spectra of Leu-Enk in aqueous and membrane-mimetic environments are shown in Fig. 2. First, as discussed in more detail below regarding the IR spectra of MPX, the peak near 1672 cm^{-1} was considered an artifact of the purification procedure [33] and was not considered in the overall analysis of the peptides. The IR spectrum of Leu-Enk in D_2O (Fig. 2A and B) was representative of that observed previously (Table 2) with an amide I maximum peak at approximately 1650 cm^{-1}; this peak did not shift significantly when the concentration of peptide was increased 10-fold from 2.7 mM to 27 mM. Unlike the previous experiments in DTPC MLVs [15], which had approximately the same lipid:peptide ratio but with 10-fold greater lipid, the amide I maximum peak for Leu-Enk in 33.2 mM DMPC MLVs (Fig. 2A) or 20 mM DCPC micelles (Fig. 2B) was not different than that observed in water. However, extreme increases in lipid concentration to 332 mM DMPC (Fig. 2A) or 484 mM DCPC (Fig. 2B) did result in a shift in the maximum amide I peak to approximately 1660 cm^{-1}. This shift was dependent strictly on lipid concentration, and independent of membrane architecture (micelle vs. bilayer) and the ratio of lipid: peptide.

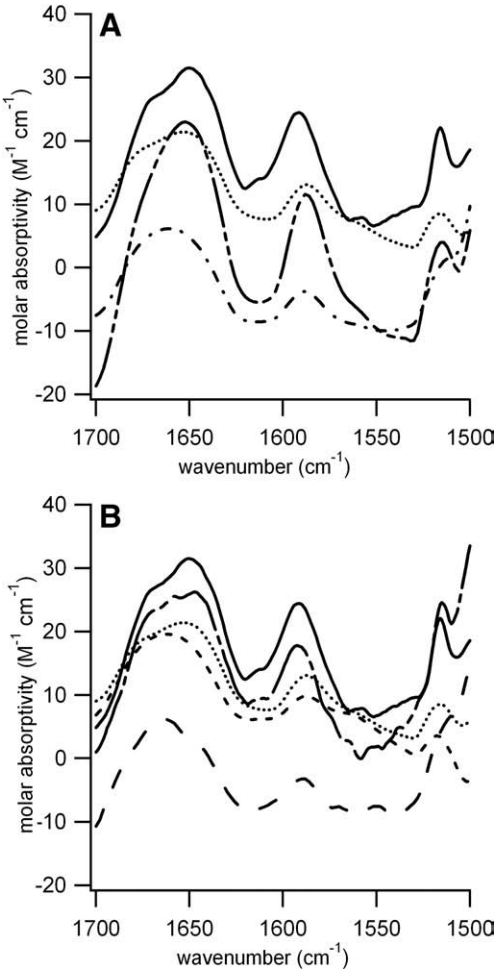

Fig. 2. IR spectra of Leu-Enk in aqueous and membrane-mimetic environments. A) 2.7 mM Leu-Enk in D_2O (solid line), 2.7 mM Leu-Enk in 33.2 mM DMPC MLVs (solid-dash–dash line), 27 mM Leu-Enk in D_2O (dotted line), and 27 mM Leu-Enk in 332 mM DMPC MLVs (dash–dot line). The ratio of lipid:peptide for both peptide concentrations was 12:1. B) 2.7 mM Leu-Enk in D_2O (solid line), 2.7 mM Leu-Enk in 20 mM DCPC micelles (broken solid line), 2.7 mM Leu-Enk in 484 mM DCPC micelles (large dashed line), 27 mM Leu-Enk in D_2O (dotted line), and 27 mM Leu-Enk in 484 mM DCPC micelles (small dashed line).

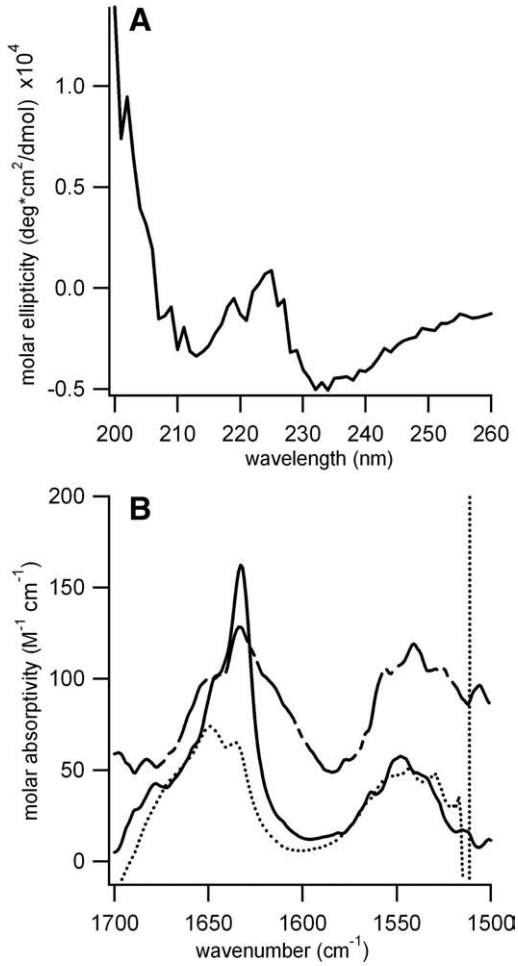

Fig. 3. A) CD spectra of 84 μM GramD in MeOH and B) IR spectra of 0.8 mM GramD in chloroform (solid line), methanol (dotted line), and 20 mM DCPC micelles (broken solid line).

3.3. GramD

The CD spectrum of GramD is shown in Fig. 3A. In methanol, GramD showed a negative molar ellipticity that qualitatively resembled that of an α-helix although the peak minima were shifted to longer wavelengths (near 213 and 233 nm, as opposed to 208 and 222 nm). These minima are characteristic of a β-helix conformation [34]. It was not possible to obtain CD spectra for GramD in the remaining solvents due to either solubility or unsuitability of the solvent for CD analysis.

As shown in Table 2, previous IR studies of GramA in chloroform and lipid bilayers showed a primary amide I peak at 1633 cm^{-1} which was assigned to β-sheet structure; additional peaks in the spectra were unassigned. Current IR spectra of GramD are shown in Fig. 3B. Compared to Table 2, the IR data in chloroform clearly reproduced results shown previously for GramA in the literature. IR spectra of GramD in 20 mM DCPC micelles was similar to those observed for the peptide in chloroform with a peak maximum at 1633 cm^{-1}. This result also agrees with previous studies of GramA in bilayers where the peak was attributed to antiparallel β-structure (Table 2). Although there was a reversal in the relative intensities for the peaks observed at 1636 and 1649 cm^{-1}, and a broad signal in the amide II region, the IR spectrum of GramD in methanol was similar to the other solvent systems tested in this study, again suggesting a similar conformation.

3.4. P16

As shown in Fig. 4A, CD spectra of P16 in TFE and 20 mM DCPC micelles showed strong CD signatures with peak minima at approximately 208 and 222 nm characteristic of α-helical secondary structure. The corresponding IR peaks in these solvents (Fig. 4B), and methanol, also had identical peak maxima in the amide I (1655 cm^{-1}) and amide II (1545 cm^{-1}) regions, again characteristic of α-helical secondary structure in a hydrophobic environment.

3.5. MPX

Fig. 5A shows CD spectra for MPX in various aqueous and membrane-mimetic solvent systems (alcohols and micelles). The membrane-mimetic solvents have previously been shown to induce helicity in MPX and can therefore be used to examine solvent effects on the IR spectrum when the same secondary structure is present. The CD signature in primarily aqueous solvents (water, 5 mM DCPC monomers) was characteristic of random coil structure while the spectra in membrane-mimicking and/or helix-inducing solvents (20 mM DCPC micelles, 50% TFE, and methanol) were α-helical. 100% TFE was unsuitable for CD analysis. Representative IR spectra for MPX in various solvent systems are shown in Fig. 5B. First, as mentioned earlier, the strong peak at 1672 cm^{-1} (and 1680 cm^{-1} in

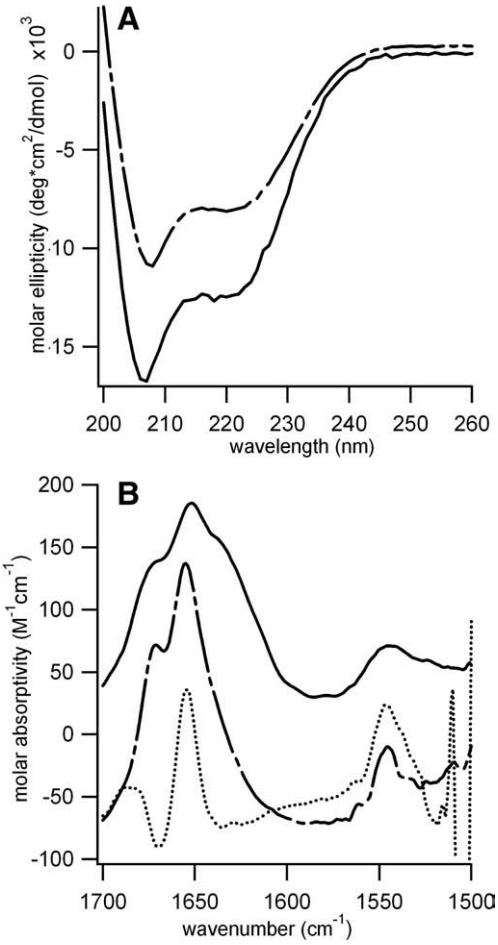

Fig. 4. A) CD spectra of 0.4 mM P16 in 50:50 TFE:H_2O (solid line) and 20 mM DCPC micelles (broken solid line) and B) IR spectra of 0.6 mM P16 in TFE (solid line), 20 mM DCPC micelles (broken solid line), and methanol (dotted line).

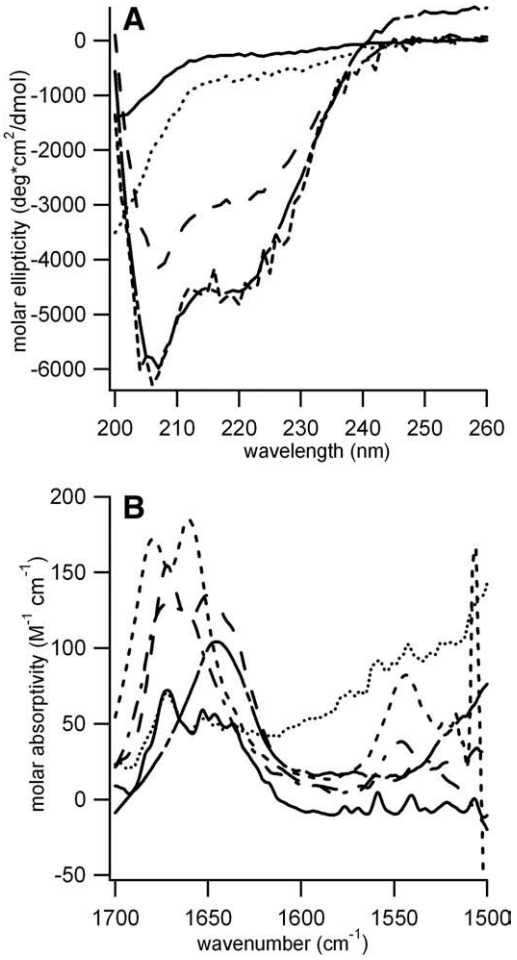

Fig. 5. A) CD spectra of MPX in water (1 mM; solid line), 5 mM DCPC monomers (0.4 mM; dotted line), 50% TFE:H_2O (0.4 mM; long dashed line), MeOH (0.4 mM; short dashed line), and 20 mM DCPC micelles (0.4 mM; broken solid line). B) IR Spectra of 1 mM MPX in D_2O (solid line), 5 mM DCPC monomers (dotted line), 50:50 TFE:D_2O (long dashed line), 100% TFE (alternating short and long dashed line), MeOH (short dashed line), and 20 mM DCPC micelles (broken solid line).

methanol) has been shown to result from residual TFA used during purification [33]. We confirmed this result in our lab by re-purifying the MPX, substituting 5 mM HCl for the 0.1% TFA typically used in the aqueous mobile phase. When MPX was purified with TFA, the peak at 1672 cm^{-1} was present (data not shown); when the peptide was re-purified with HCl, the peak at 1672 cm^{-1} was absent (as shown in Fig. 5B for MPX in 20 mM DCPC micelles). This peak was shown to shift in the alcohol solvents (data not shown). References to peak maxima, therefore, do not include this peak.

Next, based on the CD data, we expected similar IR absorption patterns, representative of random coil conformation, for MPX in D_2O and 5 mM DCPC since neither system had a membrane-like interface. As shown in Fig. 5B, both spectra were identical. However, in these spectra, there were also two additional peaks (1653 and 1637 cm^{-1}) besides the expected random coil peak at 1646 cm^{-1}. We also expected to see a distinctive shift in the IR spectra from a random coil frequency towards a helical frequency upon the addition of a membrane-mimetic solvent (alcohol) or a membrane-like interface (20 mM DCPC micelles). As shown in Fig. 5B, IR spectra in 20 mM DCPC micelles appeared to coalesce into one broader amide I maximum peak, but the location of this peak (near 1645 cm^{-1}) was not at the expected frequency of either a buried or solvent exposed α-helix (Table 1). Doubling the concentration of DCPC had no effect on the spectrum (data not shown). Compared to the IR spectrum in D_2O, addition of 50% TFE did result in a shift in the amide I peak maximum to 1650 cm^{-1}. 100% TFE and MeOH, resulted in an overall transition of over 10 cm^{-1} from a broad peak centered near 1646 cm^{-1} in D_2O to a single peak at 1662 cm^{-1}.

The amide II region for MPX (Fig. 5B) compared to the other helical peptides in 20 mM DCPC micelles (GramD in Fig. 3B and P16 in Fig. 4B) shows that GramD and P16 exhibited a distinctive absorption in this range, often seen for an α-helix (Table 1) while MPX did not. This peak was also missing for MPX in D_2O and 50% TFE/D_2O. MPX did exhibit this strong amide II stretch at 1545 cm^{-1}, in 100% TFE and methanol.

4. Discussion

4.1. Leu-Enk

As shown in Table 2, early IR studies of Leu-Enk suggested β-turn or β-sheet structure in an aqueous system [14]. More recent NMR studies have shown that Leu-Enk assumes multiple conformations in water while a more compact bent/turn structure becomes stabilized upon association with membrane-mimetics of various detergent or lipid compositions [17,35]. In addition, molecular dynamics simulations of Leu-Enk in water and dimethyl sulfoxide (DMSO) have suggested that the main difference between the β-turn and bend structures sampled by Leu-Enk is a weak hydrogen bond [16].

Although our IR spectra for 2.7 mM and 27 mM Leu-Enk in D_2O was the same as that shown previously (Table 2), the 9 cm^{-1} shift to greater wave number was not clearly present for Leu-Enk in 33.2 mM DMPC MLVs or 20 mM DCPC micelles, although the overall lipid: peptide ratio was similar. There was also no change in spectra shape

registered in the CD spectrum for Leu-Enk in 20 mM DCPC micelles. Significantly increasing the lipid concentration did induce the clear shift in the amide I IR maximum as well as a change in the shape of the overall CD spectrum. This can be explained by considering the dissociation constant (K_d) for the binding of Leu-Enk to lysophosphatidylcholine micelles, previously found to be 27 mM by NMR. This K_d was measured at a similar lipid:peptide ratio of 20:1, but with 7.6 mM Leu-Enk and 162 mM lipid) [36]. Assuming non-cooperative binding with a 1:1 binding stoichiometry (one lipid binding site on the peptide associating with one patch of lipids), this corresponded to 86% membrane-bound peptide. In the IR and CD experiments described here, 33.2 mM DMPC would correspond to only 55% of Leu-Enk being membrane-bound and 20 mM DCPC would correspond to only 42% bound. Increasing the lipid concentration to 332 mM DMPC and 484 mM DCPC would correspond to 92% and 95% peptide bound, respectively. At these higher lipid concentrations, spectral changes were clearly observed by both IR and CD. This suggests that although lipid:peptide ratios are commonly reported as experimental conditions for membrane-binding peptides, it is more important to remember that the equilibrium concentrations of bound vs. free peptide are more important for registering spectral shifts resulting from a membrane-binding event. In addition, although our results agree with previous IR analysis of Leu-Enk (Table 2), independent of membrane architecture, given the overlap of secondary assignments shown in Table 1, assignment of the IR amide I peaks to distinctive types of secondary structure should be approached with caution. This is supported by CD analysis since the resulting CD spectrum was not representative of any single type of secondary structure.

4.2. GramD

The peak minima observed by CD for GramD in methanol have been shown to be characteristic of a β-helix conformation [34]. This coincides with CD studies of GramA in 2-propanol [37] and lysolecithin bilayers [38] and with previous IR analyses of gramicidins in chloroform and lysolecithin bilayers (Table 2). Our IR spectra of GramD in chloroform and DCPC micelles also had the same amide I peak maximum (Fig. 3B). Since GramD is a hydrophobic peptide, expected to be buried within the hydrophobic interior of the micelle, it is not surprising that these solvents yielded similar spectra representative of similar structures. Some authors have suggested this β-helix conformation to be a dimeric form similar to the DNA double-helix, with intermolecular β-type hydrogen bonding between separate polypeptides [37]. Others have discounted this structure in favor of a β-helix conformation forming an end-to-end dimer with intramolecular β-strand hydrogen bonds stabilizing each individual helix [38]. Overall, for this transmembrane peptide, the CD and IR data correlated with respect to reporting on the β-type hydrogen bonding present, although analysis of the IR stretching frequencies could not be used to distinguish this β-type hydrogen bonding as a β-helix as opposed to β-sheet.

4.3. P16

CD spectra of P16 demonstrating α-helical secondary structure in 50% TFE and 20 mM DCPC micelles is in agreement with previous work [20]. Like the CD data, the IR amide I and II maxima are typical of a buried α-helix. This was expected since P16 has previously been shown to transverse the membrane [20]. In this case, the CD and IR data correlated strongly.

4.4. MPX

CD spectra of MPX revealed a definitive structural transition from random coil to α-helical conformation upon addition of a membrane-mimetic such as alcohol or 20 mM DCPC micelles. This is representative of the structural change that takes place upon transition of MPX from the free to the membrane-bound form and has been observed repeatedly throughout the literature [21–23]. However, although the CD spectra for MPX in aqueous and membrane-like systems were relatively straight forward, the IR spectra did not reveal the same trend representative of the structural transition.

IR spectra of MPX in D_2O showed multiple peaks that could be suggestive of multiple yet distinctive conformations sampled by the peptide or different levels of backbone solvation. There was no distinctive overall shift in the peak maximum upon addition of 20 mM DCPC micelles that would clearly indicate the structural transition from random coil to α-helical conformation that was observed by CD. The primary difference between the peptide spectra in D_2O and 20 mM DCPC micelles was peak broadening with less resolution of individual peaks. This result was unexpected given the presence of a 1650 cm^{-1} peak, representative of a buried or de-solvated α-helical structure, previously observed for MPX containing a non-natural amino acid IR probe in reverse-micelles [39]. However, the use of reverse-micelles is substantially different than other more common membrane-mimetics, like micelles, and could play a role in this deviation.

Our IR result in micelles could be due to stabilization of one MPX structure upon membrane-binding with the unexpected peak maximum location a result of backbone solvation. Previous work has determined the K_d for MPX to phosphatidylcholine vesicles to be approximately 42 μM [40]. As with the case of Leu-Enk, assuming a 1 peptide binding patch:1 lipid binding patch on the micelles, this corresponds to approximately 98% peptide membrane-bound at 20 mM DCPC. This in turn suggests that the observed peak broadening was representative of the helical structure and the maximum peak position at approximately 1645 cm^{-1}, that was intermediate to that expected for a buried or solvated α-helix (Table 1), was due to intermediate backbone solvation. This will be discussed further below with respect to the amide II region of the IR spectrum. Overall, the structural transition observed by CD in water compared to 20 mM DCPC micelles was not clear based on analysis of the amide I peak maximum in the IR.

Addition of 50% TFE to MPX also showed, by CD, the expected random coil to α-helix structural transition. A shift in amide I maximum frequency was also apparent in this system as well as 100% TFE. However, the 1662 cm^{-1} IR peak observed for MPX in 100% TFE is outside the limit typically observed for an α-helix, either buried or solvated (see Table 1). In fact, without complementary spectral analyses, this peak could be confused with those observed for β-turns. This result is also interesting when compared to the IR results for P16 in TFE. Both peptides have been shown by CD to form an α-helix in TFE, yet they both yielded different amide I maxima in the IR. This could be to differences in the interaction of these peptides with the solvent that occur since MPX forms an amphipathic α-helix while the P16 α-helix is entirely hydrophobic.

Amphipathicity, and hence mechanism of membrane-association may also contribute to the lack of amide II peak for MPX in the presence of micelles when compared to the other helical peptides (P16 and GramD), even though the peptide was shown by CD to be helical in micelles and 50% TFE. This could be due to deuterium exchange of the amide proton with solvent, resulting in a loss of intensity for the amide II stretch; a loss of peak intensity in the amide II region has been previously attributed to increased H–D exchange [41]. This conclusion is consistent with the other membrane-bound helices. As discussed earlier, GramD and P16 are hydrophobic and form transmembrane structures. Consequently, they displayed a strong α-helical amide II stretch at 1545 cm^{-1}. On the other hand, MPX has been shown to assume a more solvent accessible orientation when bound to the surface of a zwitterionic membrane [23]. Therefore, this amide II region could be useful in determining the degree of solvent accessibility by bound peptides.

5. Conclusion

In conclusion, IR spectroscopy is a tool for obtaining data on the secondary structure of peptides and proteins. In this work, we have performed a methodological examination of the secondary structure of four structurally diverse membrane-associating peptides. By complementing our IR experimentation with results from CD, we have shown that in some instances structural changes observed by one method (CD) are masked in the other (IR). These issues become particularly important when the membrane-bound peptide is solvent accessible as opposed to transmembrane. The amide II region of the IR spectrum may be useful in deciphering these differences in solvent accessibility. In addition, our work suggests that choice of the membrane-mimetic could also affect this.

Acknowledgements

We thank Dr. Daryl Eggers (San Jose State University) for use of his CD spectrometer and Dr. Betsy Komives (University of California San Diego) for use of her peptide synthesizer. This work was supported by a Cottrell College Science Award from Research Corporation (Tucson, AZ) and by a Faculty-Seed Start-Up Award from the California State University Program for Education and Research in Biotechnology (CSUPERB). In addition, M.M.M. was supported by a Howell Fellowship through CSUPERB.

References

[1] M. Jackson, H.H. Mantsch, The use and misuse of FTIR spectroscopy in the determination of protein structure, Crit. Rev. in Biochem. Mol. 30 (1995) 95–120.
[2] G. Martinez, G. Millhauser, FTIR spectroscopy of alanine-based peptides: assignment of the amide I' modes for random coil and helix, J. Struct. Biol. 114 (1995) 23–27.
[3] L.P. DeFlores, Z. Ganim, R.A. Nicodemus, A. Tokmakoff, Amide I'-II' 2D IR spectroscopy procides enhanced protein secondary structural sensitivity, J. Am. Chem. Soc. 131 (2009) 3385–3391.
[4] Z. Ganim, H.S. Chung, A.W. Smith, L.P. DeFlores, K.C. Jones, A. Tokmakoff, Amide I two-dimensional infrared spectroscopy of proteins, Accounts Chem. Res. 41 (2008) 432–441.
[5] G. Menestrina, Use of Fourier-transformed infrared spectroscopy for secondary structure determination of staphylococcal pore-forming toxins, in: O. Holst (Ed.), Methods in Molecular Biology, vol. 145, Humana Press Inc., Totowa, 1999.
[6] T. Miyazawa, E.R. Blout, The infrared spectra of polypeptides in aqueous solution: amide I' and amide II' bands, J. Am. Chem. Soc. 83 (1961) 712–719.
[7] W.K. Surewicz, H.M. Mantsch, New insight into protein secondary structure from resolution-enhanced infrared spectra, Biochim. Biophys. Acta 952 (1988) 115–130.
[8] W.K. Surewicz, H.M. Mantsch, D. Chapman, Determination of protein secondary structure by Fourier transform infrared spectroscopy: a critical assessment, Biochemistry 32 (1993) 389–394.
[9] H. Susi, D.M. Byler, Protein structure by Fourier transform infrared spectroscopy: second derivative spectra, Biochem. Biophys. Res. Co. 115 (1983) 391–397.
[10] S.N. Timasheff, H. Susi, L. Stevens, Infrared spectra and protein conformations in aqueous solutions, J. Biol. Chem. 242 (1967) 5467–5473.
[11] P.W. Holloway, H.H. Mantsch, Structure of cytrochrome b5 in solution by Fourier-transform infrared spectroscopy, Biochemistry 28 (1989) 931–935.
[12] T. Miyazawa, Perturbation treatment of the characteristic vibrations of polypeptide chains in various configurations, J. Chem. Phys. 32 (1960) 1647–1652.
[13] S. Krimm, J. Bandekar, Vibrational spectroscopy and conformation of peptides, polypeptides, and proteins, Adv. Protein Chem. 38 (1986) 181–364.
[14] V. Renugopalakrishnan, R. Rapaka, T. Collette, L. Carreira, R. Bhatnagar, Conformational states of leu- and met-enkephalins in solution, Biochem. Biophys. Res. Co. 126 (1985) 1029–1035.
[15] W.K. Surewicz, H.H. Mantsch, Solution and membrane structure of enkephalins as studied by infrared spectroscopy, Biochem. Biophys. Res. Co. 150 (1988) 245–251.
[16] D. van der Spoel, H.J.C. Berendsen, Molecular dynamics simulations of leu-enkephalin in water and DMSO, Biophys. J. 72 (1997) 2032–2041.
[17] C.R. Watts, M.R. Tessmer, D.A. Kallick, Structure of Leu5-enkephalin bound to a model membrane as determined by high-resolution NMR, Lett. Pept. Sci. 2 (1995) 59–70.
[18] S. Abdali, O.F. Nielsen, H. Bohr, Enkephalins: Raman spectral analysis and comparison as function of pH 1–13, Biopolymers 72 (2003) 318–328.
[19] D.A. Kelkar, A. Chattopadhyay, The gramicidin ion channel: a model membrane protein, Biochim. Biophys. Acta 1768 (2007) 2011–2025.
[20] J.A. Whiles, K.J. Glover, R.R. vold, E.A. Komives, Methods for studying transmembrane peptides in bicelles: consequences of hydrophobic mismatch and peptide sequence, J. Magn. Reson. 158 (2002) 149–156.
[21] K. Wakamatsu, A. Okada, T. Miyazawa, M. Ohya, T. Higashijima, Membrane-bound confirmation of mastoparan-X, a G-protein activating peptide, Biochemistry 31 (1992) 5654–5660.
[22] M. Seigneuret, D. Levy, A high-resolution 1H NMR approach for structure determination of membrane peptides and proteins in non-deuterated detergent: application to mastoparan X solubilized in n-octylglucoside, J. Biomol. NMR 5 (1995) 345–352.
[23] J.A. Whiles, R. Brasseur, K.J. Glover, G. Melacini, E.A. Komives, R.R. Vold, Orientation and effects of mastoparan X on phospholipid bicelles, Biophys. J. 80 (2001) 280–293.
[24] M. Bruch, Y. Crandall, Characterization of the structure and dynamics of mastoparan-X during folding in aqueous TFE by CD and NMR spectroscopy, Biopolymers 89 (2007) 197–209.
[25] J. Jonge, P. Schoen, W. terVeer, T. Stegmann, J. Wilschut, A. Huckriede, Use of a dialyzable short-chain phospholipid for efficient solubilization and reconstitution of influenza virus envelopes, Biochim. Biophys. Acta 1758 (2006) 527-236.
[26] W. Reisdorf, S. Krimm, Infrared amide I' band of the coiled coil, Biochemistry 35 (1996) 1383–1386.
[27] G.A. Jeffrey, An Introduction to Hydrogen Bonding, University Press, New York, 1997.
[28] E.S. Manas, Z. Getahun, W. Wright, W.F. DeGrado, J.M. Vanderkooi, Infrared spectra of amide groups in α-helical proteins: evidence for hydrogen bonding between helices and water, J. Am. Chem. Soc. 122 (2000) 9883–9890.
[29] R.N.A.H. Lewis, E.J. Prenner, L.H. Kondejewski, C.R. Flach, R. Mendelsohn, R.S. Hodges, R.N. McElhaney, Fourier transform infrared spectroscopic studies of the interaction of the antimicrobial peptide gramicidin S with lipid micelles and with lipid monolayer and bilayer membranes, Biochemistry 38 (1999) 15193–15203.
[30] M.M. Palian, V.I. Boguslavsky, D.F. O'Brien, R. Polt, Glycopeptide-membrane interactions: glycosyl enkephalin analogues adopt turn conformations by NMR and CD in amphipathic media, J. Am. Chem. Soc. 125 (2003) 5823–5831.
[31] D.M. Byler, H. Susi, Examination of the secondary structure of proteins by deconvolved FTIR spectra, Biopolymers 25 (1986) 469–487.
[32] C.L. Wilder, A.D. Friedrich, R.O. Potts, G.O. Daumy, M.L. Francoeur, Secondary structural analysis of two recombinant murine proteins, interleukins 1alpha and 1beta: is infrared spectroscopy sufficient to assign structure? Biochemistry 31 (1992) 27–31.
[33] H. Gaussier, H. Morency, M.C. Lavoie, M. Subirade, Replacement of trifluoroacetic acid with HCl in the hydrophobic purification steps of pediocin PA-1: a structural effect, Appl. Environ. Microb. 68 (2002) 4803–4808.
[34] N.D. Lazo, D.T. Downing, Beta-helical fibrils from a model peptide, Biochem. Biophys. Res. Co. 235 (1997) 675–679.
[35] I. Chandrasekhar, W.F. van Gunsteren, G. Zandomeneghi, P.T.F. Williamson, B.H. Meier, Orientation and conformational preference of leucine-enkephalin at the surface of a hydrated dimyristoylphosphatidylcholine bilayer: NMR and MD simulation, J. Am. Chem. Soc. 128 (2006) 159–170.
[36] C. Deber, B. Behnam, Role of membrane lipids in peptide hormone function: binding of enkephalins to micelles, Proc. Natl. Acad. Sci. U. S. A. 81 (1984) 61–65.
[37] W. Veatch, E. Fossel, E.R. Blout, The conformation of gramicidin A, Biochemistry 13 (1974) 5249–5256.
[38] D. Urry, R. Shaw, T. Trapane, K. Prasad, Infrared spectra of the gramicidin A transmembrane channel: the single-stranded beta-6 helix, Biochem. Biophys. Res. Co. 114 (1983) 373–379.
[39] S. Mukherjee, P. Chowdhury, W. DeGrado, F. Gai, Site-specific hydration status of an amphipathic peptide in AOT reverse micelles, Langmuir 23 (2007) 11174–11179.
[40] A. Arbuzova, G. Schwarz, Pore-forming action of mastoparan peptides on liposomes: a quantitative analysis, Biochim. Biophys. Acta 1420 (1999) 139–152.
[41] X. Han, G. Li, G. Li, K. Lin, FTIR study of the thermal denaturation of α-actinin in its lipid-free and dioleoylphosphatidylglycerol-bound states and the central and n-terminal domains of α-actin in D2O, Biochemistry 37 (1998) 10730–10737.
[42] Y.N. Chirgadze, N.A. Nevskaya, Infrared spectra and resonance interaction of amide-I vibration of the parallel-chain pleated sheet, Biopolymers 15 (1976) 627–636.
[43] J.M. Purcell, H. Susi, Solvent denaturation of proteins as observed by resolution-enhanced Fourier transform infrared spectroscopy, J. Biochem. Biophys. Methods 9 (1984) 193–199.
[44] N.A. Nevskaya, Y.N. Chirgadze, Infrared spectra and resonance interactions of amide-I and II vibrations of alpha-helix, Biopolymers 15 (1976) 637–648.
[45] R.J. Jakobsen, L.L. Brown, T.B. Hutson, D.J. Fink, A. Veis, Intermolecular interactions in collagen self-assembly as revealed by Fourier transform infrared spectroscopy, Science 220 (1983) 1288–1290.
[46] D.M. Vu, J.K. Myers, R. Oas, R.B. Dyer, Probing the folding and unfolding dynamics of secondary and tertiary structures in a three-helix bundle protein, Biochemistry 43 (2004) 3582–3589.
[47] C. Huang, J.W. Klemke, Z. Getahun, W.F. DeGrado, F. Gai, Temperature-dependent helix-coil transition of an alanine based peptide, J. Am. Chem. Soc. 123 (2001) 9235–9238.
[48] M. Jackson, P.I. Haris, D. Chapman, Conformational transitions in poly(L-lysine)-studies using Fourier transform infrared spectroscopy, Biochim. Biophys. Acta 998 (1989) 75–79.
[49] M. Pezolet, S. Bonenfant, F. Dousseau, Y. Popineau, Conformation of wheat gluten proteins, FEBS Lett. 299 (1992) 247–250.